PDSS2 Methylation Exacerbates Heart Failure through Inhibition of the CXCL14/NF- κ B Signaling Pathway

Liyan Yu¹, Shuxia Cai¹, Xiuli Guo^{1,*}

¹Department of Gerontology, Yantaishan Hospital, 264000 Yantai, Shandong, China

*Correspondence: wcbgxl@126.com (Xiuli Guo)

Published: 1 May 2024

Background: Numerous reports have suggested a correlation between the occurrence of heart failure (HF) and the methylation status of specific key genes in myocardial cells. This study aimed to elucidate the mechanistic role and functional impact of the methylation of pentenyl diphosphate synthase subunit 2 (*PDSS2*) methylation in HF, offering insights for novel therapeutic approaches in HF management.

Methods: The HF rat model was established via surgical intervention to explore the *in vivo* exacerbation of HF by *PDSS2* methylation. Cardiac ultrasound and morphological assessments were used to evaluate HF in rat hearts. Hematoxylin-eosin (HE) staining was used to assess cardiac injury. The levels of *PDSS2* methylation and expression were quantified, and the underlying mechanisms of *PDSS2* in HF pathogenesis were explored.

Results: Our findings revealed a significant reduction in *PDSS2* levels in the heart tissue of HF rats (p < 0.05), concurrent with a notable increase in *PDSS2* methylation (p < 0.05). Decreased *PDSS2* methylation led to the upregulation of nuclear factor-kappaB (NF- κ B) expression (p < 0.05) and chemokine (C-X-C motif) ligand 14 (*CXCL14*) levels (p < 0.05), consequently attenuating myocardial tissue damage in HF rats. However, silencing CXCL14 or administering the NF- κ B inhibitor BAY 11-7082 reversed the protective effects of 5-Aza-2'-deoxycytidine (5-Aza) (p < 0.05), thus increasing myocardial tissue damage in HF rats.

Conclusion: *PDSS2* methylation is a significant contributor to cardiac dysfunction and the progression to heart failure, underscoring its potential importance in the therapeutic landscape of HF.

Keywords: *PDSS2*; methylation; NF- κ B p65; CXCL14; heart failure

Introduction

The incidence of heart failure (HF) is increasing globally, emerging as a significant public health concern. HF affects approximately 20% of the global population, with an associated mortality rate of 11%. Clinical medicine recognizes HF as a complex syndrome with elevated risks [1]. Declining cardiac function and left ventricular dilatation are primary contributors to hospitalization and mortality in HF patients. Biomarkers such as brain natriuretic peptide (BNP) and atrial natriuretic peptide (ANP), indicative of fetal gene expression, play crucial roles in the clinical diagnosis and prognosis of HF [2]. Currently, inhibition of neuroendocrine stimulation remains the primary therapeutic approach for HF. However, it fails to prevent the ultimate progression of the disease [3]. Therefore, there is a pressing need to explore alternative and more effective therapeutic strategies.

The pathogenesis of HF is closely intertwined with epigenetic modifications. Unlike genetic alterations, epigenetic mechanisms offer promising avenues for HF therapy due to the reversible nature and heritability of chromatin modifications [4]. Deoxyribonucleic acid (DNA) methylation and microRNA are intricately involved in the dys-

regulated expression observed in HF [5]. DNA methylation silences or activates genes, regulating cardiovascular diseases (CVDs). Pentenyl diphosphate synthase subunit 2 (*PDSS2*), discovered in 2005, exhibits anti-tumor effects in various malignancies. For example, Chen *et al.* [6] demonstrated that forced overexpression of *PDSS2* affected the cell cycle, leading to apoptosis in gastric cancer (GC) cell lines. In addition, abnormal *PDSS2* levels may induce DNA damage in the liver, contributing to the onset and progression of hepatocellular carcinoma (HCC) [7]. Kanda *et al.* [8] revealed that the hypermethylation of the *PDSS2* promoter influenced *PDSS2* expression in GC cells, impacting GC development. However, the impact of *PSDD2* promoter methylation on HF and its underlying mechanism needs further investigation.

Chemokine (C-X-C motif) ligand 14 (CXCL14) is a member of the CXC chemokine family [9]. The CXC chemokine superfamily has the effect of regulating inflammation and autoimmunity [10]. Zeng L *et al.* [11] demonstrated that the methylation of Iroquois homeobox 1 (IRX1) suppresses CXCL14 expression, promoting HF development. CXCL14 plays a crucial role in the inflammatory cascade, with nuclear factor-kappaB (NF- κ B) signaling be-

ing a pivotal mediator of the inflammatory response [12]. Therefore, it is plausible to hypothesize that CXCL14 activates the NF- κ B pathway. Study by Wente *et al.* [13] demonstrated that CXCL14 upregulates nuclear NF- κ B p65 expression, promoting invasion in pancreatic cancer cells. Furthermore, IRX1 methylation enhances lung metastasis of osteosarcoma by regulating the CXCL14/NF- κ B signaling pathway [14]. Interestingly, Zeng *et al.* [7] observed that *PDSS2*-Del2 overexpression in hepatocellular carcinoma (HCC) cells inhibited fumarate levels and activated the canonical NF- κ B pathway. Therefore, we propose that *PDSS2* methylation may exacerbate HF development through the CXCL14/NF- κ B signaling pathway.

In this study, we established an HF rat model and evaluated various cardiac function indicators and PDSS2 expression and methylation levels. Employing cell transfection and the methylation inhibitor 5-Aza-2'-deoxycytidine (5-Aza) to regulate PDSS2 expression and methylation levels, respectively, we assessed alterations in cardiac function indicators and the activation of CXCL14/NF- κ B pathway. Our findings reveal the impact of PDSS2 methylation on HF and its underlying association with the CXCL14/NF- κ B pathway. The results of this study offer a promising advancement in understanding the role of PDSS2 in HF and provide a potential biomarker for HF diagnosis and treatment.

Materials and Methods

Animal Experimental Groups

Healthy male Sprague-Dawley (SD) rats (180 \pm 20 g, n = 60) were procured from Yantaishan Hospital of Shandong Province. The rats were housed in a pathogen-free animal facility with controlled conditions (temperature: 20 \pm 2 °C, humidity: 40–70%), providing ad libitum access to food and water.

The rat models were established according to the previously reported method [15]. Briefly, the HF rat model was induced by ligating the left atrial appendage and left pulmonary artery, while sham-operated rats underwent coronary artery exposure and suture threading without ligation. One month post-surgery, HF modeling was confirmed by a left ventricular ejection fraction (LVEF) ≤45% measured using echocardiography (MYLABTM X5 VET, Esaote, Genoa, Italy) [16,17]. Moreover, to determine the impact of PDSS2 or CXCL14 on HF, the negative control short hairpin (sh)RNA (sh-NC) and the shRNA against PDSS2 (sh-PDSS2) or against CXCL14 (sh-CXCL14) was obtained (order no. GOSE0497639, GeneChem, Shanghai, China) and was used for gene knockdown (2 \times 10¹² vg per rat) according to the manufacturer's instruction. The experimental design comprised 10 groups, including: Control (n = 6), sham (n = 6), HF (n = 6), HF+sh-NC (n =6), HF+sh-NC+5-Aza (1 mg/kg, intraperitoneal injection; 189625, Sigma-Aldrich, Shanghai, China) (n = 6), HF+5Aza (n = 6), HF+sh-PDSS2 (n = 6), HF+sh-PDSS2+5-Aza (n = 6), HF+sh-CXCL14+5-Aza (n = 6), and HF+5-Aza+BAY 11-7082 (5 mg/kg, intraperitoneal injection; HY-13453, MedChemExpress, Monmouth Junction, NJ, USA) (n = 6). The sequences of short hairpin RNAs were listed in Table 1. Control rats were injected with phosphate-buffered saline (PBS; 10 μ L; C0221, Beyotime, Shanghai, China) [18]. This experimental protocol was approved by the Ethics Committee of Yantaishan Hospital of Shandong Province (approval no. 2021043).

Left Ventricular Echocardiography and Heart Hemodynamics in HF Rats

Following anesthesia induction using pentobarbital sodium (50 mg/kg; P3761, Sigma-Aldrich, Bellefonte, PA, USA) via intraperitoneal injection, relevant indices were assessed using Doppler ultrasonography (DC-26, Mindray Medical, Shenzhen, China) and a multi-channel physiological recorder (MP160, BIOPAC, Wageningen, Holland).

Ventricular Mass Index in HF Rats

Rats were euthanatized with pentobarbital sodium (180 mg/kg; P3761, Sigma-Aldrich, Bellefonte, PA, USA) through intraperitoneal injection. The rat hearts were extracted and divided into the left and right ventricles. Subsequently, the right and left ventricular masses were measured using electronic balance. Left ventricular muscle mass index (LVMI) and right ventricular myocardial infarction (RVMI) were determined by calculating the ratio of ventricular mass to body weight.

Hematoxylin-Eosin (HE) Staining

Heart tissues were sectioned and stained with hematoxylin (C0105S, Beyotime, Shanghai, China) for 10 min. Subsequently, sections were treated with 1% hydrochloric acid ethanol (53219460, SINOPHARM, Shanghai, China) and Scott's Bluing Solution (G1865, Solarbio, Beijing, China). After tissues were washed with distilled water, eosin staining (C0105S, Beyotime, Shanghai, China) was performed for 3 min. The stained tissues were observed and photographed using an optical microscope (NE930, Jiangnan Yongxin Optics, Nanjing, China).

Promoter Region of PDSS2

The nucleotide sequence encompasses a 200-bp DNA region characterized by a high GC content (>50%) and an observed cytosine-guanine (CpG) to expected CpG ratio (CpG/Expected CpG) \geq 0.6 within the *PDSS2* promoter region. This evaluation determined the presence or absence of CpG islands. The positions of CpG islands were determined using CpG Island Searcher software (https://www.labtools.us/cpg-island-searcher/) [19].

Name	Sequences (5'-3')
sh-PDSS2-F	GATCCCCACCATAATTTGAGGCCTATCTCGAGATAGGCCTCAAATTATGGTGGTTTTTG
sh-PDSS2-R	AATTCAAAAACCACCATAATTTGAGGCCTATCTCGAGATAGGCCTCAAATTATGGTGGG
sh-CXCL14-F	GATCCGCACCAAGCGCTTCATCAATTCAAGAGATTGATGAAGCGCTTGGTGCTTTTTTGG
sh-CXCL14-R	AATTCCAAAAAAGCACCAAGCGCTTCATCAATCTCTTGAATTGATGAAGCGCTTGGTGCG
sh-NC-F	GATCCACCGGCCTAAGGTTAAGTCGCCCTCGCTCGAGCGAG
sh-NC-R	AATTCAAAAAACCGGCCTAAGGTTAAGTCGCCCTCGCTCG

sh-*PDSS2*, shRNA against *PDSS2*; *PDSS2*, pentenyl diphosphate synthase subunit 2; sh-*CXCL14*, shRNA against *CXCL14*; *CXCL14*, chemokine (C-X-C motif) ligand 14; sh-*NC*, negative control shRNA; F, forward; R, reverse.

Quantitative Real-Time Reverse Transcription Polymerase Chain Reaction (qRT-PCR)

Tissue homogenates were mixed with Trizol reagent (DP424, Tiangen Biochemical Technology (Beijing) Co., Ltd., Beijing, China) to extract total RNA. Subsequently, the RNA was reverse transcribed using TaqMan reagent to generate complementary DNA (cDNA). The target gene was amplified by PCR in a 50 μ L reaction system. Actin served as an internal reference gene for *PDSS2*. The relative expression of genes was determined using the $2^{-\Delta \Delta Ct}$ method. Table 2 presents the primer sequence for fluorescence quantification.

Table 2. Sequence of the primers for fluorescence quantification.

quantification.		
Primer sequences (5'-3')		
CACCAAGAGCGTGTCCAG		
CTCGTTCCAGGCGTTGTA		
TGCCGAGTGAACCGAAAC		
TGGTGCTCAGGGATGACG		
AGTGTCAGAGGCGGAGAA		
CTGTGGTAAGCAGAGGGT		
GACGCCCTCCGATGTGAAAG		
GGCTCTGTTACTGCTTAGTTCAA		
CAGAAGGTGCTGCCCCAGATG		
GACTGCGCCGATCCGGTC		
ACACTGTGCCCATCTACG		
TGTCACGCACGATTTCC		

NF- κB , nuclear factor-kappaB; ANP, atrial natriuretic peptide; BNP, brain natriuretic peptide; hum, human; F, forward; R, reverse.

Methylation-Specific PCR (MSP)

Genomic DNA was extracted following the protocol outlined in the Genomic DNA Extraction Kit insert (DP304, Tiangen Biochemical Technology, Beijing, China). Subsequently, the DNA was amplified through PCR using ITS universal primers, as detailed in the amplification system highlighted in Table 3. The reaction procedure was 95 °C, 5 min, 94 °C, 20 s, 60 °C, 30 s, 35 cycles, 72 °C, 20 s, 72

 $^{\circ}$ C, 5 min, 35 cycles. Following the reaction, 10 μ L of the reaction product was analyzed using 1% agarose gel electrophoresis. The agarose gel electropherogram was quantified by scanning the band grayscale using ImageJ software (version 1.48, National Institutes of Health, Rockville, MD, USA) [20].

Table 3. Sequence of the primers.

Name	Primer sequences (5'-3')
PDSS2 Left M primer	GATTTTTCGATATTATTTTTTCGG
PDSS2 Right M primer	ATAACGACGTTACTAAACTCGTCG
PDSS2 Left U primer	AGATTTTTTGATATTATTTTTTTGG
PDSS2 Right U primer	TAACAACATTACTAAACTCATCACT
GAPDH-F	TGTCTCCTGCGACTTCAACA
<i>GAPDH-</i> R	GGTGGTCCAGGGTTTCTTACT

GAPDH, glyceraldehyde-3-phosphate dehydrogenase.

Global DNA Methylation Measurement

Genomic DNA was extracted from the left ventricle and treated with phosphodiesterase I, Benzonase, and shrimp alkaline phosphatase. Methylcytosine (Cm) and cytosine (C) levels were determined using high-performance liquid chromatography (HPLC) coupled with tandem mass spectrometry (HPLC-MS, G6465BA, Agilent, Santa Clara, CA, USA). The results were expressed as the Cm/C ratio [21].

Western Blot Assay

Proteins were extracted on ice using the protease-inhibitor cocktail (P0013J, Beyotime, Shanghai, China) for 10 minutes. After centrifugation at 12,000 g for 10 minutes, the supernatant was collected, and the protein concentration was quantified using the BCA kit (P0010S, Beyotime, Shanghai, China). Subsequently, proteins were separated using 10% SDS-PAGE gels (P0012A, Beyotime, Shanghai, China) and transferred to polyvinylidene fluoride (PVDF) membranes (YA1701, Solarbio, Beijing, China). The membranes were then incubated overnight at 4 °C with primary antibodies against PDSS2 (1:1000, A16557, Abclonal, Wuhan, China), CXCL14 (1:1000, 10468-1-AP,

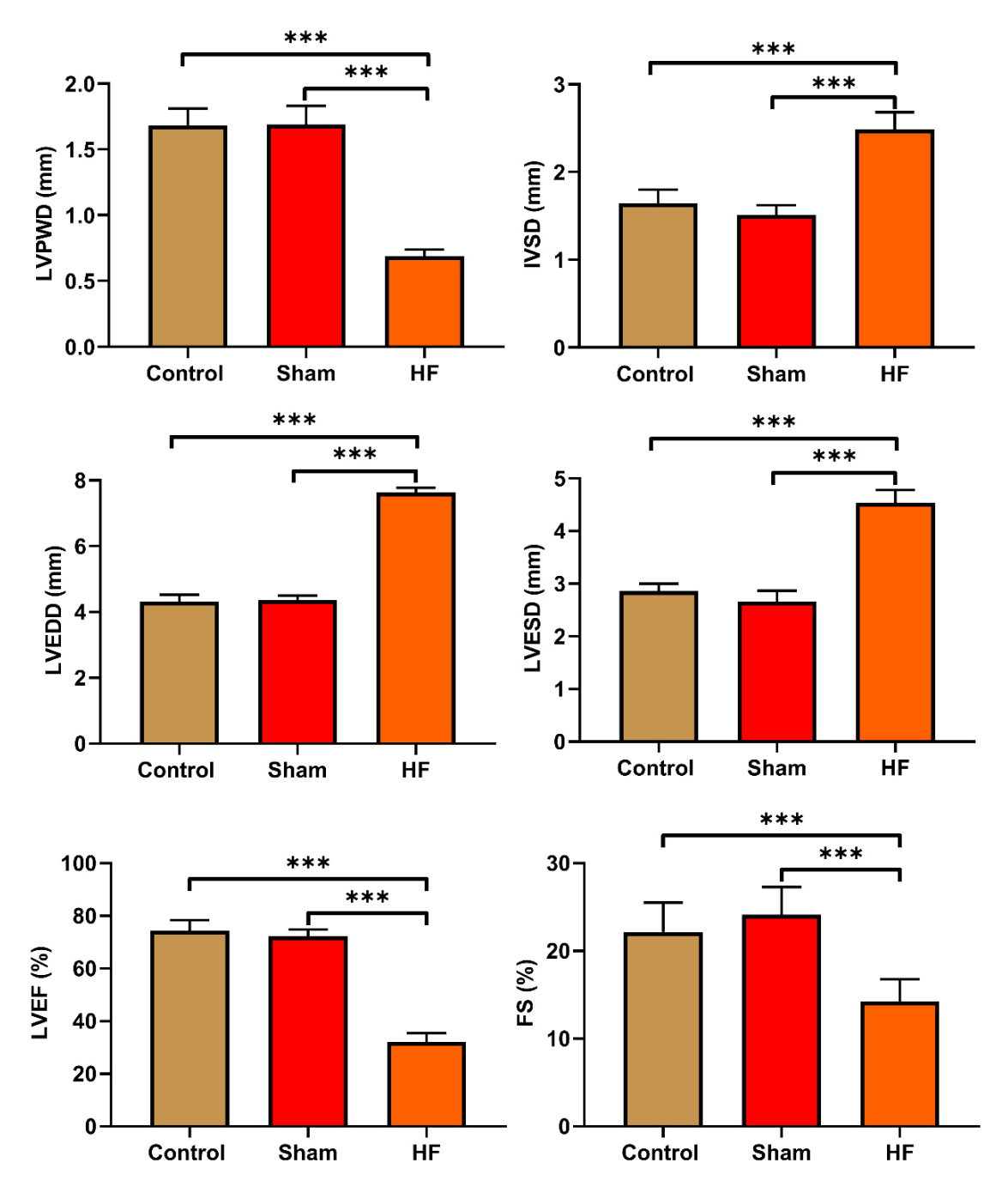


Fig. 1. Echocardiographic data in rats. n = 6, ****p < 0.001. HF, heart failure; LVPWD, left ventricular posterior wall thickness; IVSD, interventricular septal dimension; LVEDD, left ventricular end-diastolic diameter; LVESD, left ventricular end-systolic diameter; LVEF, left ventricular ejection fraction; FS, fractional shortening.

Proteintech, Wuhan, China), NF-κB p65 (1:1000, A2547, Abclonal, Wuhan, China), and glyceraldehyde-3-phosphate dehydrogenase (GAPDH) (1:20,000, AC001, Abclonal, Wuhan, China). Following incubation with secondary antibody (1:10,000, AS003, Abclonal, Wuhan, China) at room temperature for 1 hour, the membranes were visualized using the WBKLS0500 developer (MILLIPORE, Billerica, MA, USA) and imaged using the Tanon 5200 system (Tanon, Shanghai, China) according to the standard laboratory protocols [22].

Statistical Analysis

Data analysis was performed using GraphPrism 8.0.2 software (GraphPad Software Inc., San Diego, CA, USA, https://www.graphpad-prism.cn/). Results were presented as Mean \pm standard deviation (SD). One-way analysis of variance (ANOVA) or two-tailed Student's *t*-test was used to evaluate differences among groups, followed by Bonferroni's post hoc analysis. A *p*-value < 0.05 was considered statistically significant.

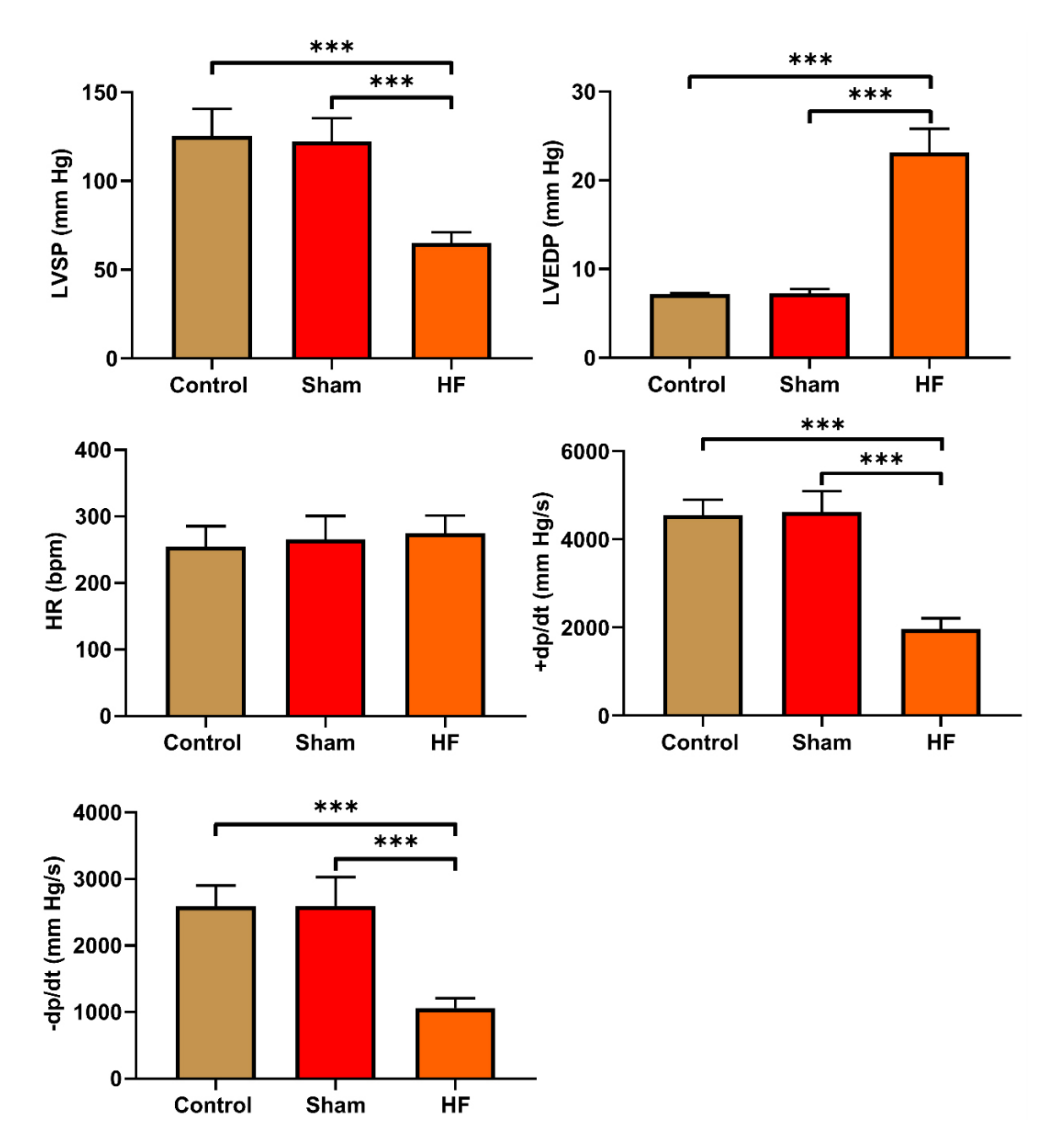


Fig. 2. Cardiac hemodynamic parameters in rats. n = 6, ***p < 0.001. LVSP, left ventricular systolic pressure; LVEDP, left ventricular end-diastolic pressure; HR, heart rate; +dp/dt, rate of increase in left ventricular pressure; -dp/dt, rate of decrease in left ventricular pressure.

Results

Characterization of HF Rats

Fig. 1 illustrates that HF exhibited elevated levels of interventricular septal dimension (IVSD) at end-diastole, left ventricular end-diastolic diameter (LVEDD), and left ventricular end-systolic diameter (LVESD), and decreased levels of left ventricular posterior wall thickness (LVPWD) at end-diastole, left ventricular ejection fraction (LVEF), and fractional shortening (FS) compared to control or sham rats (p < 0.001). Additionally, Fig. 2 demonstrates a sig-

nificant increase in left ventricular end-diastolic pressure (LVEDP) and a marked reduction in left ventricular systolic pressure (LVSP), as well as rate of increase in left ventricular pressure (+dp/dt) and rate of decrease in left ventricular pressure (-dp/dt), in the HF group compared to control and sham groups (p < 0.001). Furthermore, the levels of left ventricular muscle mass index (LVMI) and right ventricular myocardial infarction (RVMI) were higher in HF rats compared to control and sham groups (Fig. 3A,B, p < 0.01). Moreover, Fig. 3C,D show that atrial natriuretic peptide (ANP) and brain natriuretic peptide (BNP) mRNA ex-

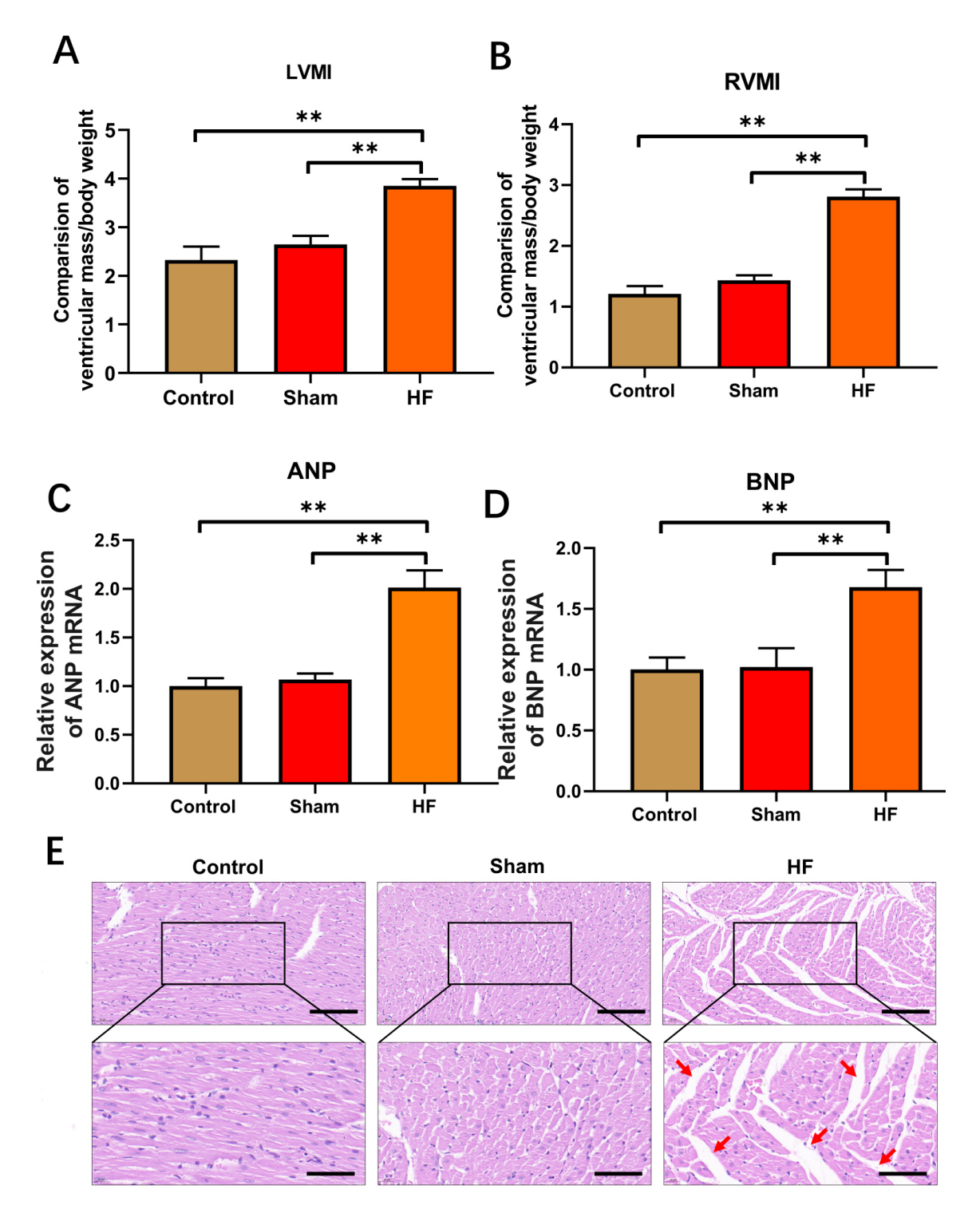


Fig. 3. Characterization of heart failure (HF) in rats. (A,B) Ventricular mass indices were determined by calculating the ratio of ventricular mass to body weight. Expression of ANP (C) and BNP (D) in cardiac tissues was detected using qRT-PCR. (E) HE staining of cardiac tissues from control, sham, and HF rats with morphological changes was indicated by red arrows (scale bar: $100 \mu m$, $50 \mu m$). n = 6, **p < 0.01. qRT-PCR, quantitative real-time reverse transcription polymerase chain reaction; HE, hematoxylin-eosin; LVMI, left ventricular muscle mass index; RVMI, right ventricular myocardial infarction.

pressions were upregulated in the HF group (p < 0.01). HE staining revealed disordered arrangement and increased interstitial spaces between muscle fibers of cardiomyocytes in HF hearts (Fig. 3E; indicated by red arrows).

PDSS2 mRNA Expression and Methylation Status in Cardiac Tissues of HF Rats

Fig. 4A illustrates that the CpG island contained 1655 bp, with a GC content of 55.9% and an observed

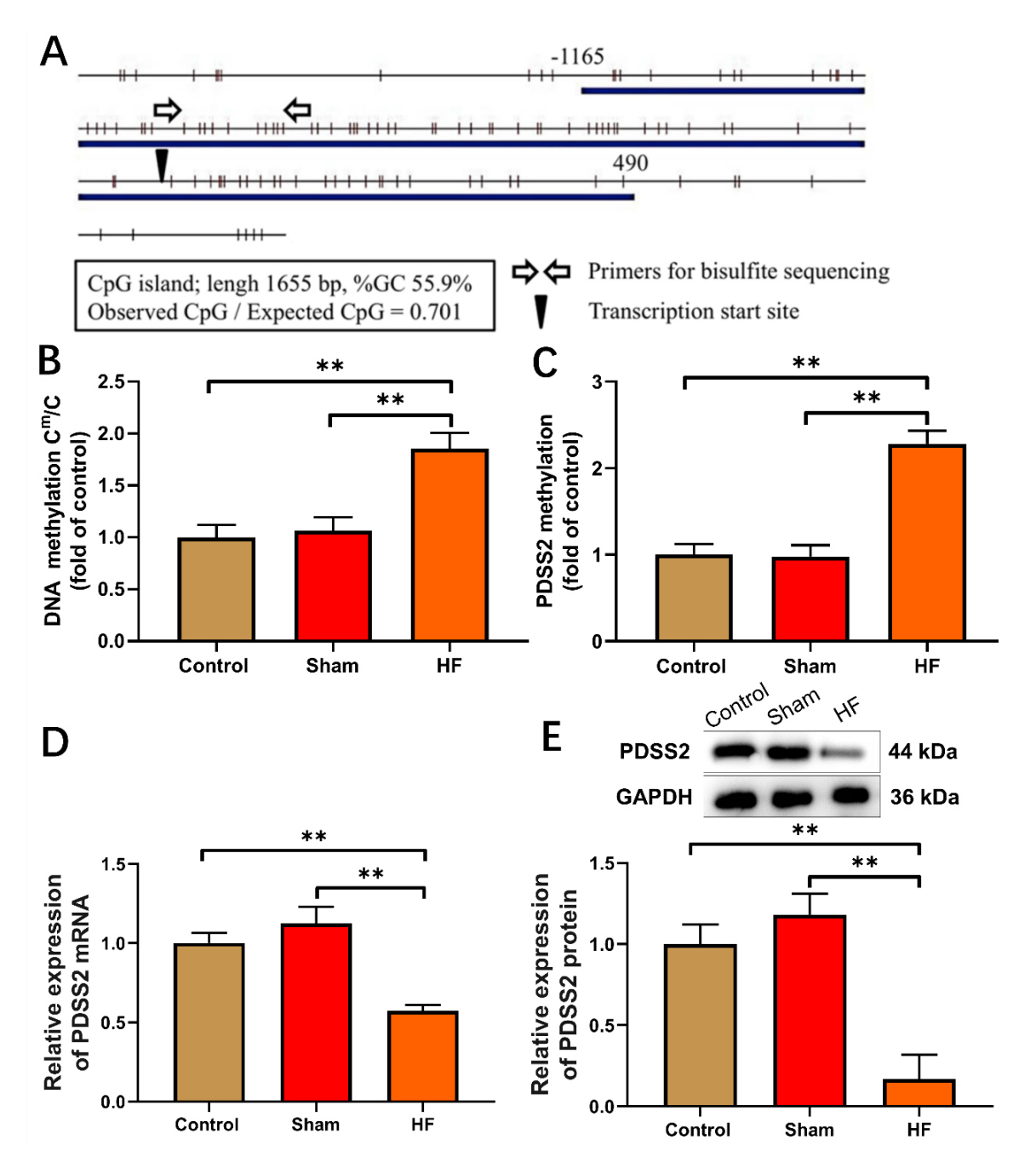


Fig. 4. *PDSS2* expression and methylation in HF rats. (A) Observation of a cytosine-guanine (CpG) island. (B) Analysis of global deoxyribonucleic acid (DNA) methylation in cardiac tissues using high-performance liquid chromatography coupled with tandem mass spectrometry (HPLC-MS). (C) Detection of *PDSS2* methylation in cardiac tissues using methylation-specific PCR. (D) Quantification of *PDSS2* mRNA expression in cardiac tissues using qRT-PCR. (E) Detection of PDSS2 protein levels in cardiac tissues using Western blot analysis. n = 6, **p < 0.01.

CpG/expected CpG ratio of 0.70. Therefore, we hypothesized that hypermethylation of the CpG islands affects PDSS2 expression. As illustrated in Fig. 4B,C, HF promoted global genomic DNA methylation and a genespecific PDSS2 methylation (p < 0.01). Moreover, the levels of PDSS2 mRNA (Fig. 4D, p < 0.01) and protein (Fig. 4E, p < 0.01) were suppressed in the left ventricle of HF rats.

CXCL14/NF-κB p65 Pathway in Cardiac Tissues of HF Rats

CXCL14 and NF- κ B signaling pathways participated in the inflammatory response and may be regulated by *PDSS2* methylation. As illustrated in Fig. 5A,C, the levels of *NF-\kappaB* mRNA and NF- κ B p65 protein did not show significant differences between the control and sham groups but decreased significantly in HF rats (p < 0.01). More-

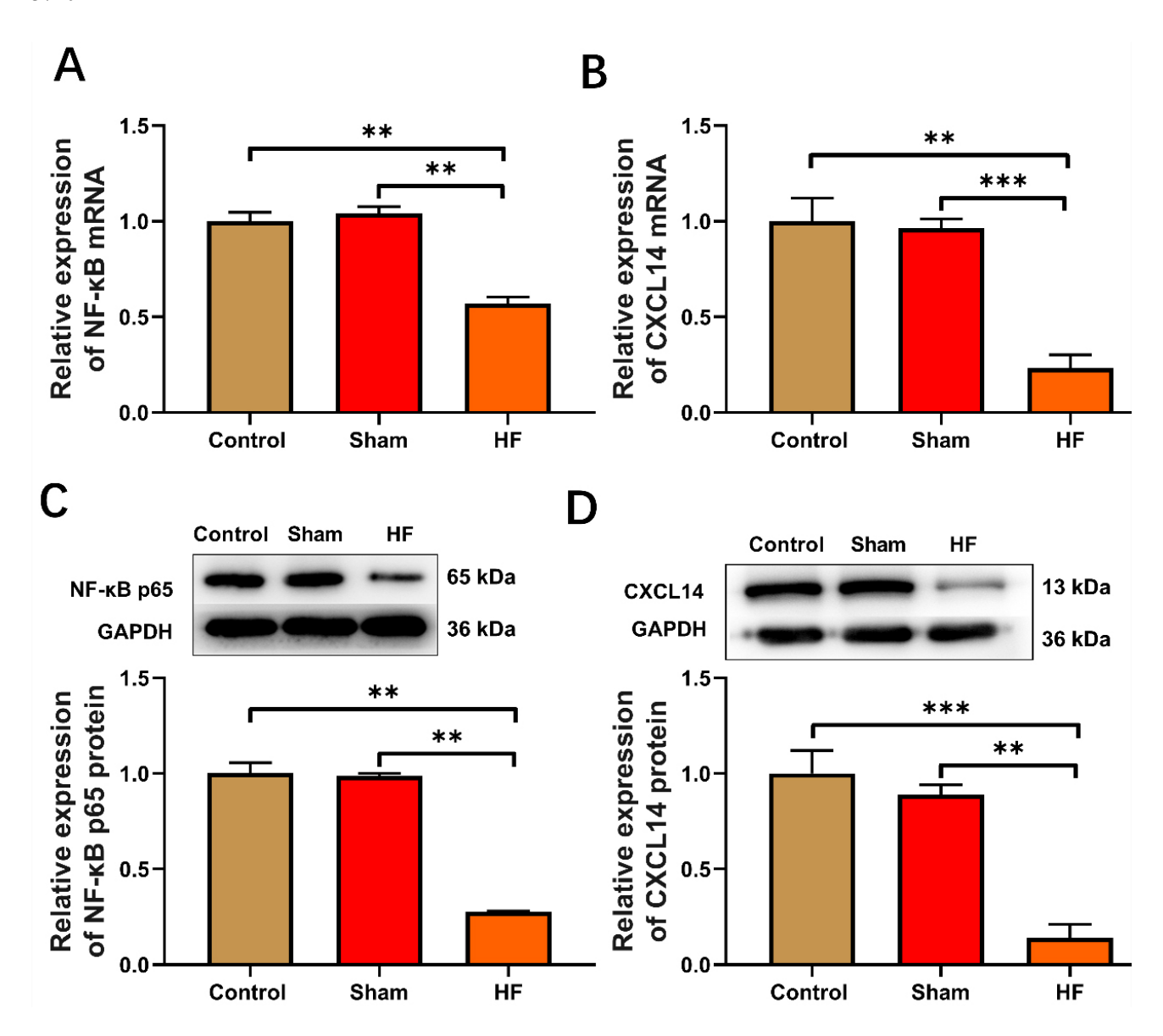


Fig. 5. CXCL14/NF- κ B p65 pathway is involved in the occurrence of HF. mRNA levels of NF- κ B (A) and CXCL14 (B) in cardiac tissues were quantified by qRT-PCR. Protein expressions of NF- κ B p65 (C), and CXCL14 (D) in cardiac tissues were analyzed by Western blot analysis. n = 6, **p < 0.01, ***p < 0.001.

over, the level of CXCL14 was markedly reduced in HF rats (p < 0.01, Fig. 5B,D), consistent with the *PDSS2* trend observed earlier.

5-Aza Suppresses PDSS2 Hypermethylation and Consequently Restores PDSS2 Expression in HF Rats, and sh-PDSS2 Successfully Reduces PDSS2 Expression

Compared to the HF+sh-NC or HF+sh-PDSS2 group, significantly increased PDSS2 expression and decreased PDSS2 DNA methylation were observed in HF rats treated with 5-Aza (p < 0.01, Fig. 6A,B). These findings indicate that 5-Aza effectively inhibits PDSS2 methylation and restores PDSS2 expression, which is significant for alleviating HF. Moreover, Fig. 6C–E demonstrate that PDSS2 is less expressed in HF+sh-PDSS2 (compared to HF+sh-PDSS2)

NC; p < 0.01) and in HF+sh-PDSS2+5-Aza (compared to HF+sh-NC+5-Aza; p < 0.001), indicating successful sh-PDSS2 transfection.

Reduced PDSS2 Expression Induced by sh-PDSS2 Exacerbates HF, while Increased PDSS2 Induced by PDSS2 Methylation Inhibition Ameliorates HF

The cardiac function and hemodynamics of rats in each group were measured, and the results are presented in Figs. 7,8, respectively. It was observed that 5-Aza induced lower levels of IVSD, LVEDD, LVESD, and LVEDP (p < 0.001) while exhibiting higher levels of LVPWD, LVEF, FS, LVSP, +dp/dt, and -dp/dt (p < 0.001). In contrast, sh-PDSS2, which decreased PDSS2 expression, led to higher levels of IVSD, LVEDD, LVESD, and LVEDP (p < 0.001) while showing lower levels of LVPWD, LVEF, FS, LVSP,

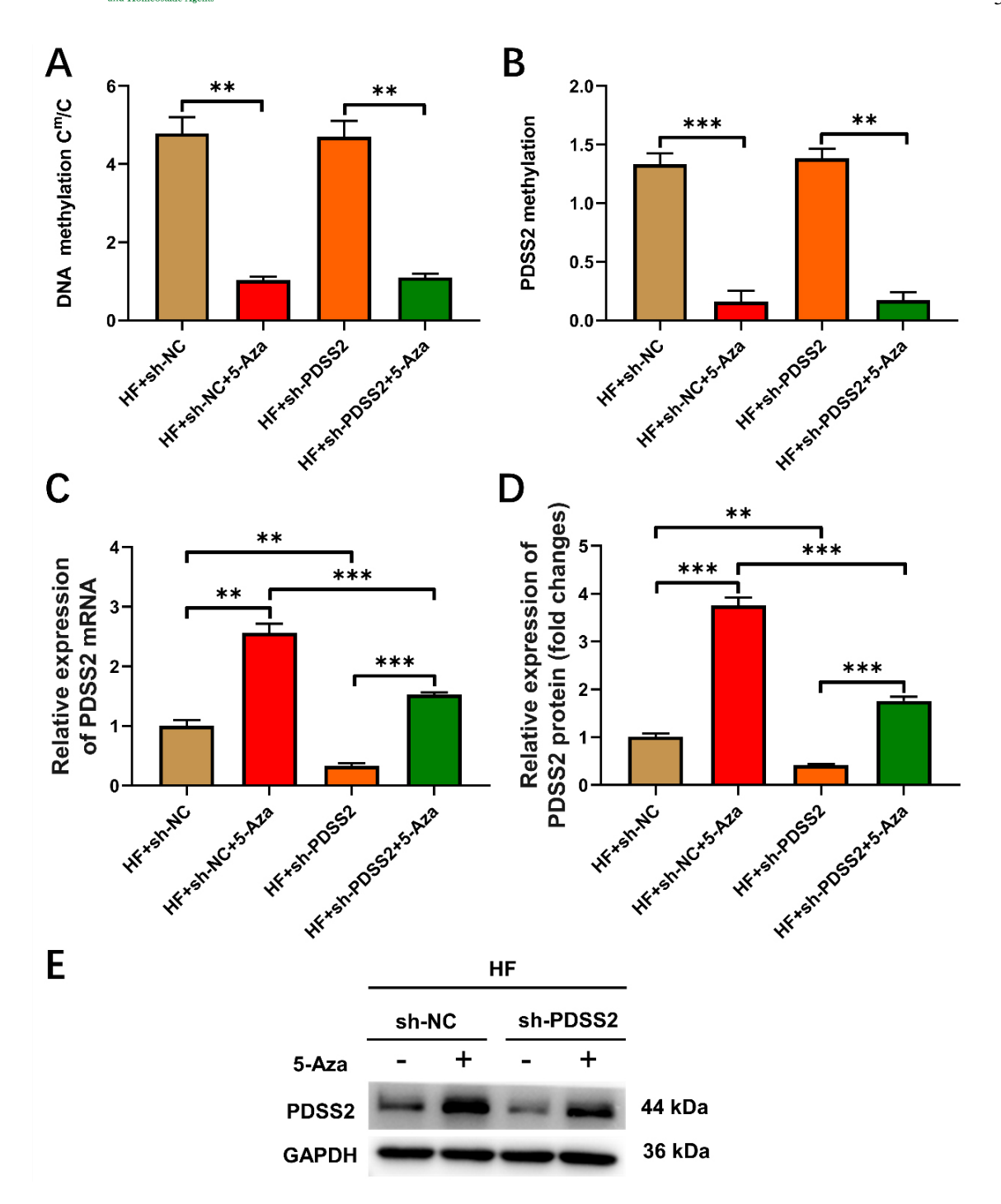


Fig. 6. 5-Aza-2'-deoxycytidine (5-Aza) suppresses *PDSS2* hypermethylation and restores PDSS2 expression, while sh-*PDSS2* reduces *PDSS2* expression in HF rats. (A) Global DNA methylation in cardiac tissues was quantified using HPLC-MS. (B) *PDSS2* methylation in cardiac tissues was assessed using methylation-specific PCR. (C) *PDSS2* mRNA expression in cardiac tissues was quantified using qRT-PCR. (D,E) PDSS2 protein levels in cardiac tissues were determined by Western blot analysis. n = 6, **p < 0.01, ***p < 0.001.

+dp/dt, and -dp/dt (p < 0.001). Furthermore, it was observed that 5-Aza induced lower levels of ANP mRNA, BNP mRNA, LVMI, and RVMI (Fig. 9A–D, p < 0.01), whereas sh-PDSS2 led to higher levels of ANP mRNA, BNP mRNA, LVMI, and RVMI (Fig. 9A–D, p < 0.05). Additionally, histological analysis via HE staining revealed that

tissue samples from the HF+sh-NC or HF+sh-PDSS2 group exhibited more disordered arrangement and larger spaces of cardiomyocytes, which were effectively improved by 5-Aza-induced PDSS2 methylation inhibition (Fig. 9E; indicated by red arrows). These findings corroborate that decreased PDSS2 levels could exacerbate heart failure, and

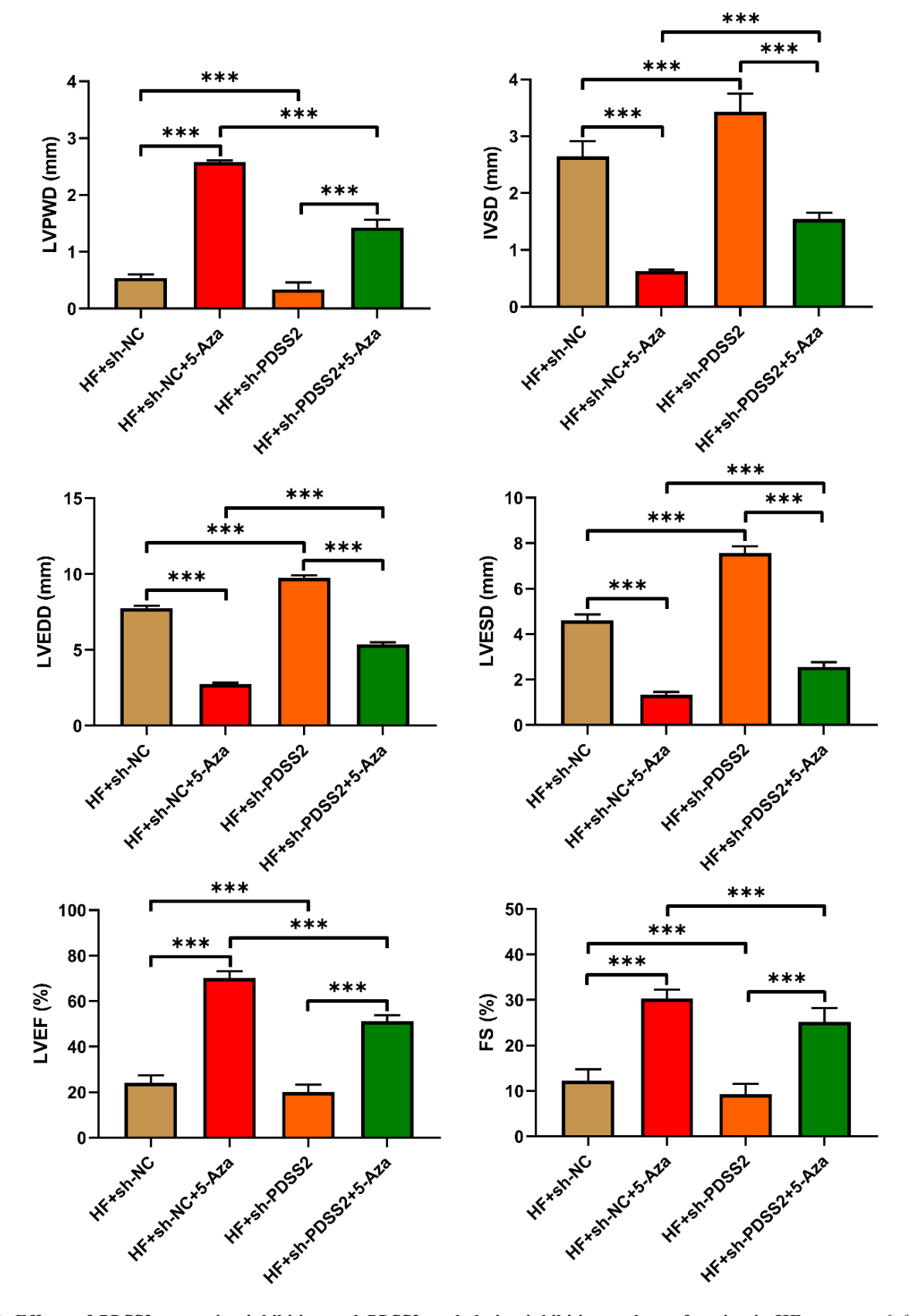


Fig. 7. Effects of *PDSS2* expression inhibition and *PDSS2* methylation inhibition on heart function in HF rats. n = 6, *** p < 0.001.

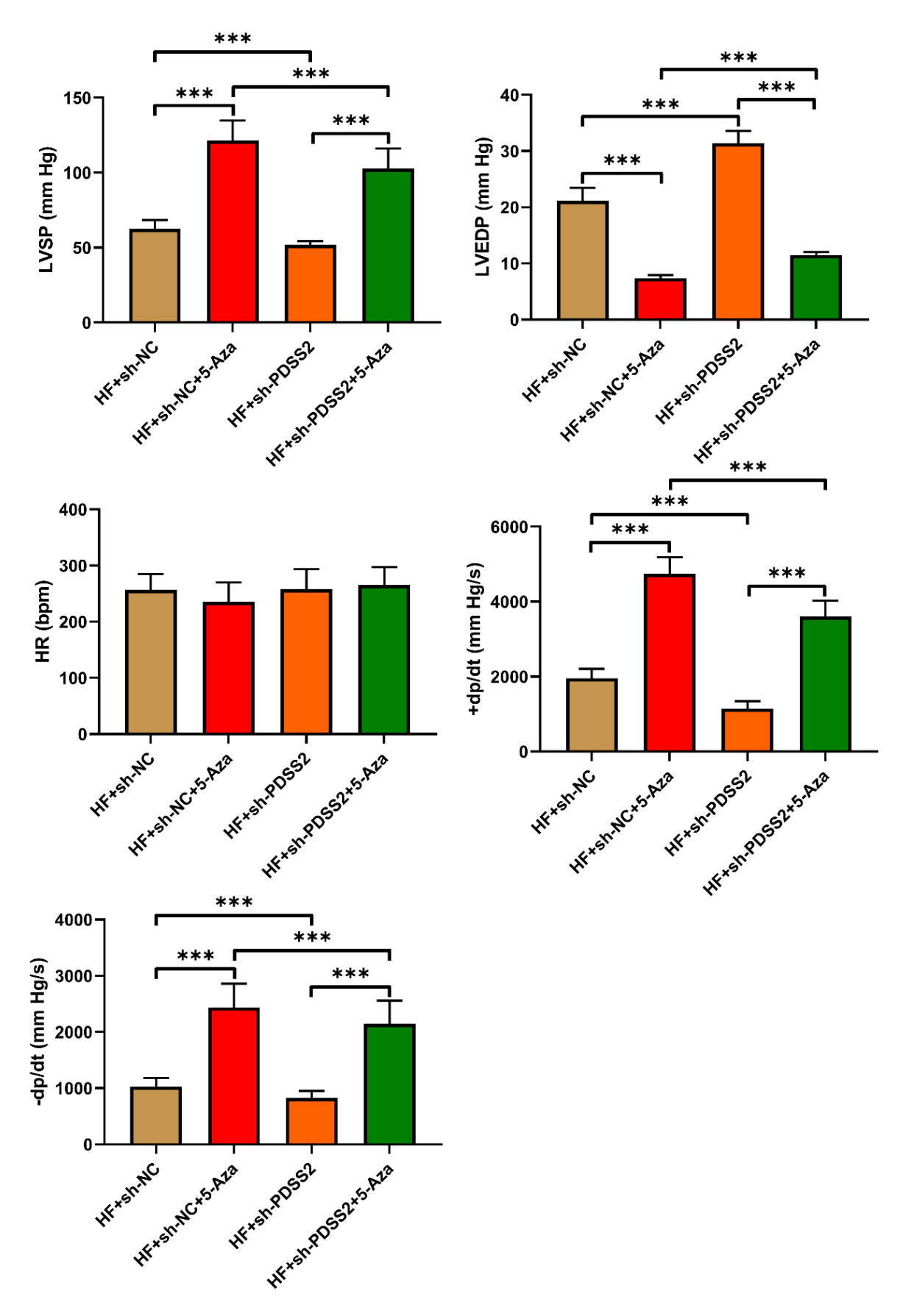


Fig. 8. Effects of *PDSS2* expression inhibition and *PDSS2* methylation inhibition on heart hemodynamics in HF rats. n = 6, *** p < 0.001.

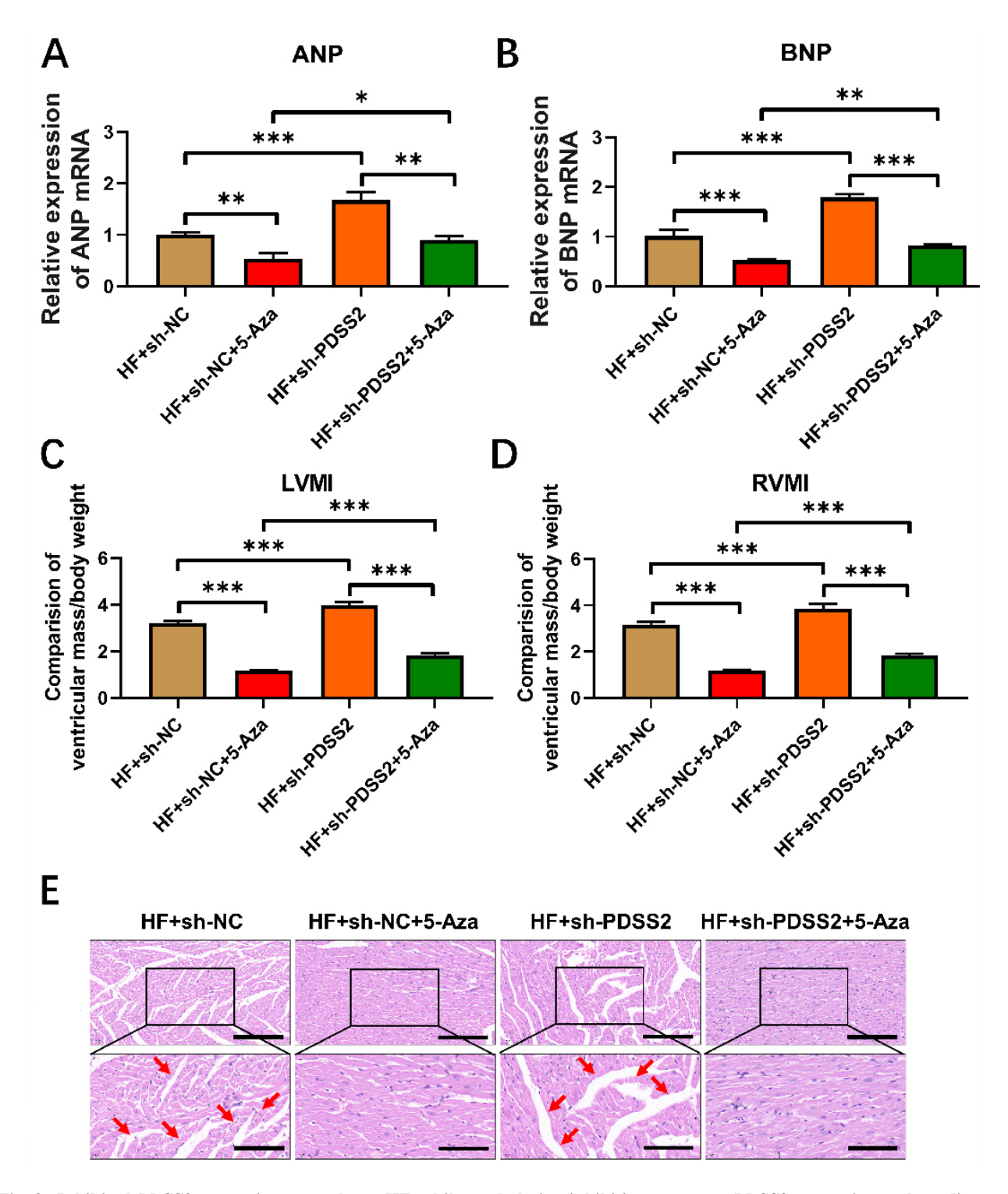


Fig. 9. Inhibited *PDSS2* expression exacerbates HF, while methylation inhibition promotes *PDSS2* expression and ameliorates HF in rats. Expressions of *ANP* (A) and *BNP* mRNAs (B) in cardiac tissues were quantified using qRT-PCR. (C,D) Ventricular mass indices were calculated by determining the ratio of ventricular mass to body weight. (E) HE staining of cardiac tissue (red arrows indicate morphological changes; scale bar: $100 \mu m$, $50 \mu m$). n = 6, *p < 0.05, **p < 0.01, ***p < 0.001.

the 5-Aza-induced decrease in *PDSS2* methylation and increase in *PDSS2* expression levels could ameliorate heart failure.

Inhibition of PDSS2 Methylation Ameliorates HF by Activating the CXCL14/NF-κB Signal Pathway

It was hypothesized that PDSS2 methylation influences the CXCL14/NF- κ B pathway. Therefore, further investigation was warranted to elucidate the potential mech-

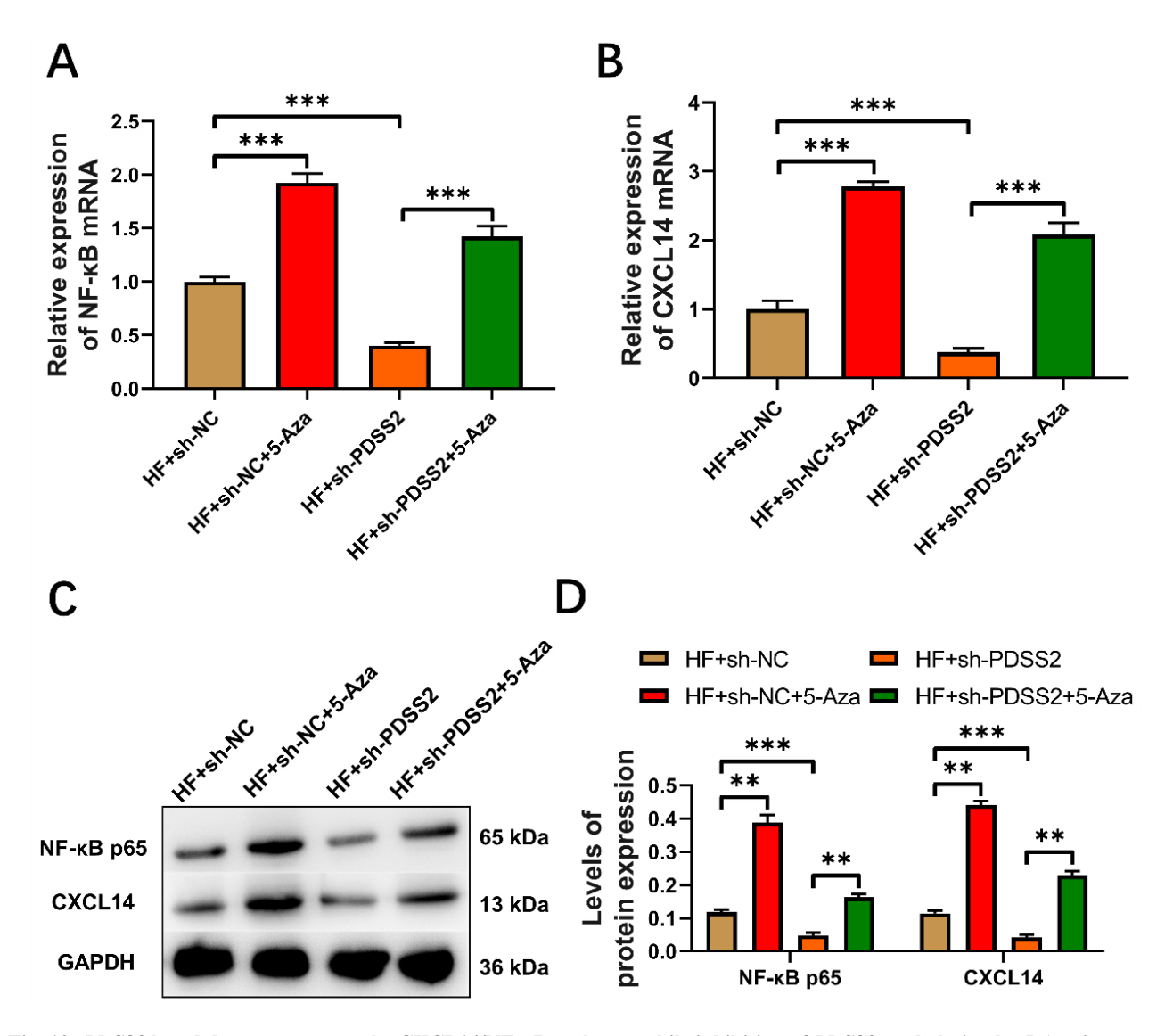


Fig. 10. *PDSS2* knockdown suppresses the CXCL14/NF- κ B pathway, while inhibition of *PDSS2* methylation by 5-Aza increases the activation of the CXCL14/NF- κ B signal pathway. NF- κ B and CXCL14 mRNA and protein expressions in cardiac tissues were quantified using qRT-PCR (A,B) and Western blot analysis (C,D). n = 6, **p < 0.01, ***p < 0.001.

anism of 5-Aza-induced *PDSS2* methylation in HF rats. The study revealed that in 5-Aza-treated cell groups (where *PDSS2* methylation was inhibited and *PDSS2* expression was restored), the levels of NF- κ B and CXCL14 were significantly increased (Fig. 10A–D, p < 0.01). Conversely, PDSS2 knockdown by sh-*PDSS2* resulted in decreased NF- κ B p65 and CXCL14 (Fig. 10A–D, p < 0.001). These findings, in conjunction with previous experimental results, confirmed that the inhibition of *PDSS2* methylation induced by 5-Aza and the subsequent increase in *PDSS2* expression contributed to the effective alleviation of HF through activation of the CXCL14/NF- κ B pathway.

Moreover, Fig. 11A illustrated that continued administration of 5-Aza to inhibit *PDSS2* methylation, coupled with the successful knockdown of CXCL14 (p < 0.001), led to decreased levels of *NF-\kappaB* (p < 0.001) and increased levels of *ANP* (p < 0.001) and *BNP* (p < 0.001). Furthermore,

Fig. 11B–D demonstrated that inhibited PDSS2 methylation reduced LVMI (p < 0.001), RVMI (p < 0.001), and pathological changes of heart tissues, which were all reversed by suppression of the CXCL14/NF- κ B pathway (p < 0.001). These findings revealed that 5-Aza-induced PDSS2 methylation inhibition and subsequent increase in PDSS2 expression ameliorated HF only when the CXCL14/NF- κ B pathway was successfully activated.

NF-\(\kappa B\) Inhibitor Reverses the Protective Effect of 5-Aza-Induced PDSS2 Methylation Inhibition

Fig. 12A illustrates that compared to the HF group, CXCL14 expression was upregulated (p < 0.001) when HF+5-Aza treatment was used to inhibit PDSS2 methylation. Concurrently, the expression levels of NF- κB were also upregulated (p < 0.001), while the levels of ANP (p < 0.001) and BNP (p < 0.001), associated with heart fail-

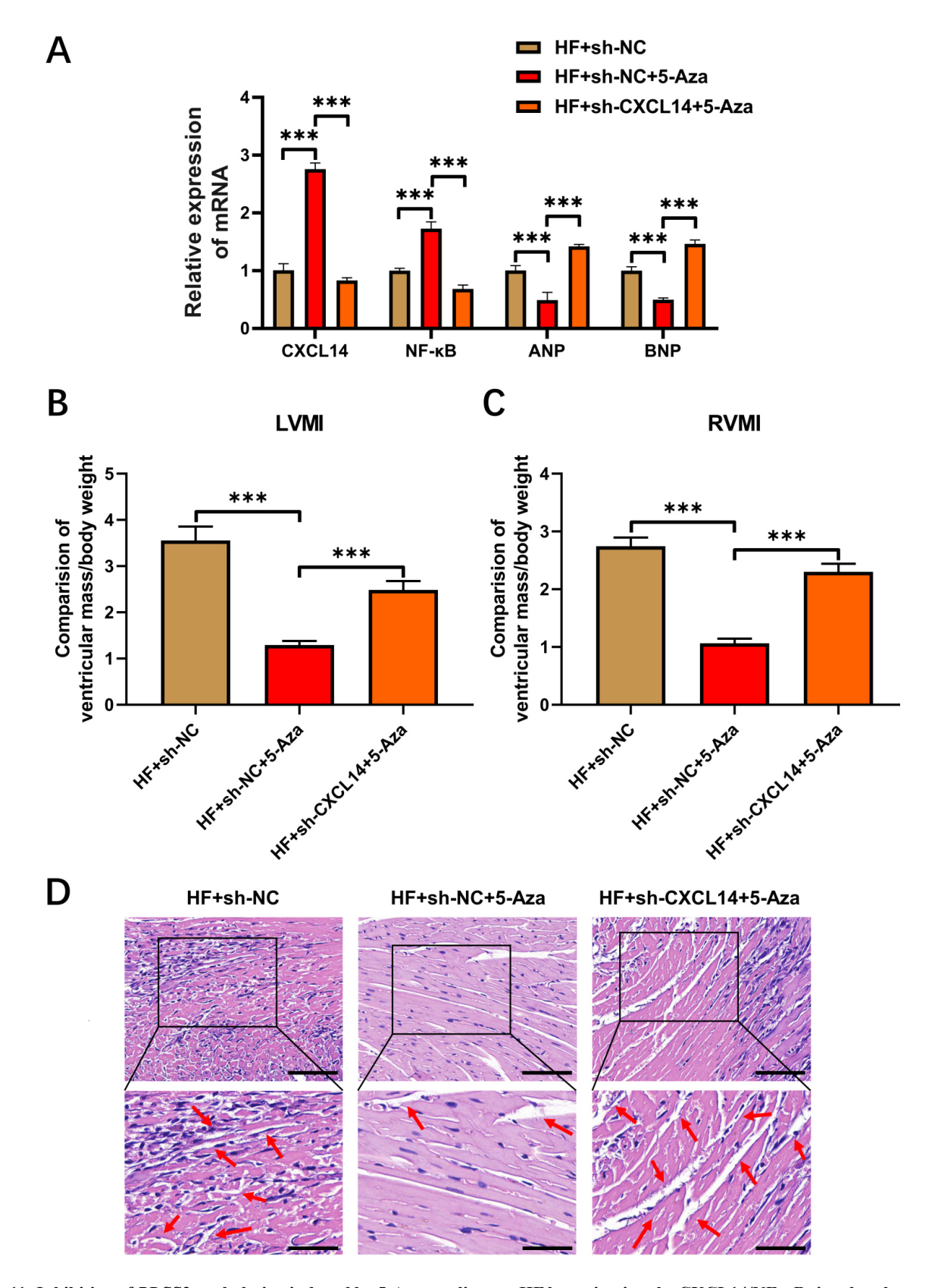


Fig. 11. Inhibition of *PDSS2* methylation induced by 5-Aza ameliorates HF by activating the CXCL14/NF- κ B signal pathway. (A) mRNA levels of *CXCL14*, *NF*- κ B, *ANP*, and *BNP*. (B,C) Ventricular mass indices were determined by calculating the ratio of ventricular mass to body weight. (D) HE staining of cardiac tissue (red arrows indicate morphological changes; scale bar: 50 μ m, 20 μ m). n = 6, ***p < 0.001.

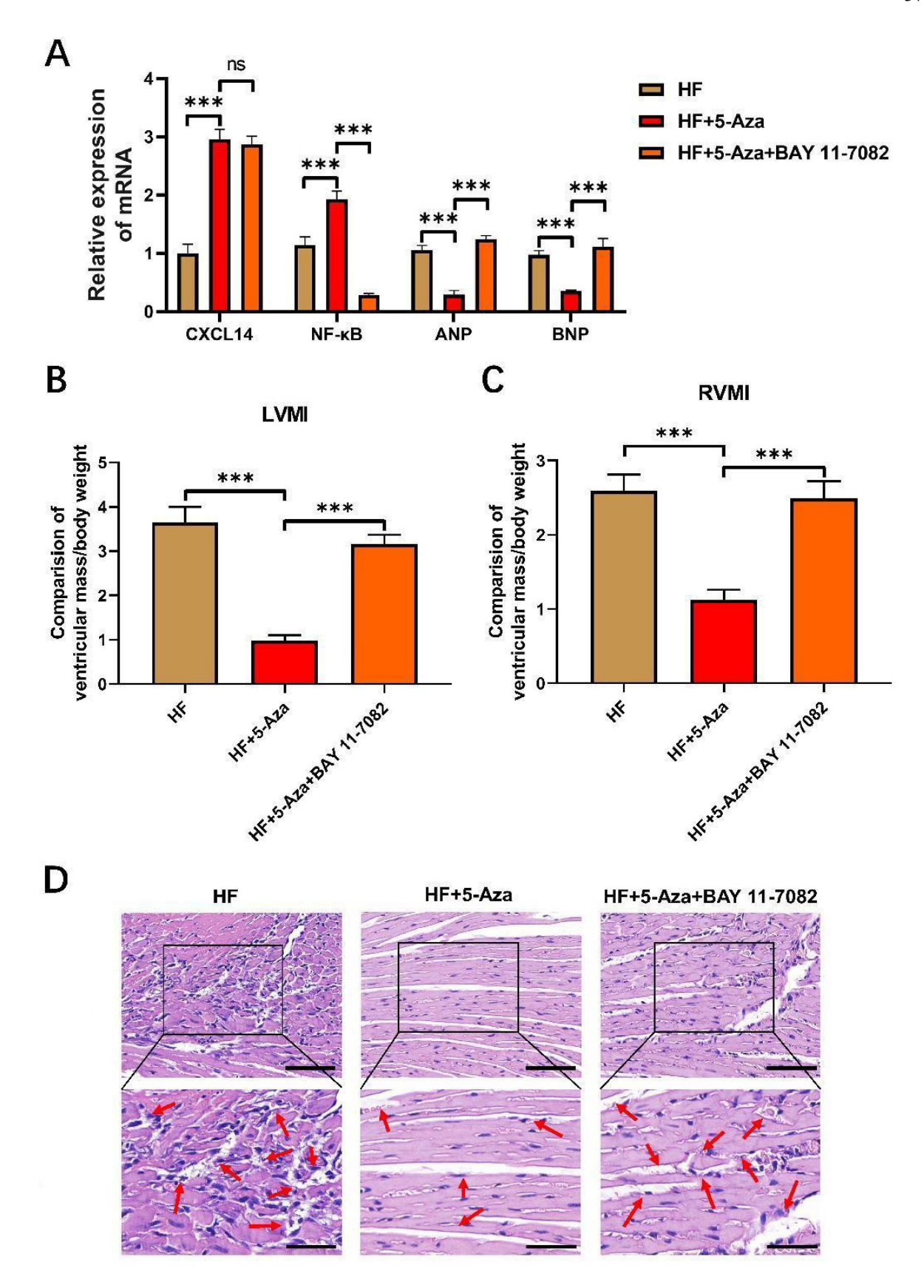


Fig. 12. NF- κ B inhibitor reverses the protective effect of 5-Aza-induced PDSS2 methylation inhibition. (A) mRNA levels of *CXCL14*, *NF-\kappaB*, *ANP*, and *BNP*. (B,C) Ventricular mass indices were assessed by calculating the ratio of ventricular mass to body weight. (D) HE staining of cardiac tissue (red arrows indicate morphological changes; scale bar: 50 μ m, 20 μ m). n = 6, ***p < 0.001; ns, no significance.

ure, were decreased. However, compared to the HF+5-Aza treatment group, applying the NF- κB -specific inhibitor HF+5-Aza+BAY 11-7082 decreased NF- κB expression. Furthermore, the expression levels of ANP (p < 0.001) and BNP (p < 0.001) were upregulated. Additionally, Fig. 12B–D demonstrate a decrease in LVMI (p < 0.001) and RVMI (p < 0.001) and an amelioration of pathological changes after inhibiting PDSS2 methylation to improve HF. Nevertheless, the inhibition of the NF- κ B signaling pathway further enhanced the reversal of LVMI (p < 0.001) and RVMI (p < 0.001). These findings suggest that the inhibition of 5-Aza-induced PDSS2 methylation and the subsequent elevation in PDSS2 expression contribute to the improvement of HF, particularly when the CXCL14/NF- κ B pathway is effectively activated.

Discussion

Heart failure is a complex condition characterized by numerous yet unexplored underlying causes and mechanisms. Various animal and cell models have been developed to mimic HF [23,24]. This study aimed to investigate the role of PDSS2 methylation in HF and its potential mechanism by affecting the CXCL14/NF- κ B signaling pathway. In this investigation, we utilized a rat model of arterial ligation to simulate HF disease and assessed relevant cardiac function parameters. Our results indicated significant cardiac function and hemodynamics differences between HF rats and normal controls. HF rats exhibited elevated levels of IVSD, LVEDD, LVESD, LVEDP, LVMI, and RVMI and decreased levels of LVPWD, LVEF, FS, LVSP, +dp/dt, and -dp/dt compared to control or sham rats. Additionally, ANP and BNP mRNA expressions were increased in the HF group, and histological analysis via HE staining revealed disordered cardiomyocyte arrangement, confirming the successful establishment of the HF rat model.

Pentenyl diphosphate synthase subunit 2 (PDSS2) is a pivotal enzyme in Coenzyme Q10 (CoQ10) synthesis, an essential component of the mitochondrial electron transport chain and crucial for cardiomyocytes energy metabolism. The methylation status of *PDSS2* modulates its enzymatic activity, influencing CoQ10 synthesis and cardiomyocyte energy metabolism. Epigenetic regulation, particularly DNA methylation, plays a crucial role in disease onset and progression. To understand the role of epigenetics in gene expression and cellular phenotype, a high-throughput sequencing or array platform focusing on methylation of gene promoter CpG island has facilitated genome-wide methylation markers analysis [25]. In line with these observations, we identified a CpG island in the PDSS2 promoter region using CpG island searching tools, suggesting that hypermethylation of CpG island regulates PDSS2 expression in HF rats. Our study revealed significantly reduced PDSS2 gene expression with a tendency towards methylation in the HF rat model. Significantly reduced levels of CXCL14 and NF-

κB were detected in HF rats compared to the control group, significantly impacting HF onset and progression. Kanda et al. [26] demonstrated reduced PDSS2 mRNA expression and hypermethylation of the PDSS2 promoter in liver cancer tissues. Moreover, PDSS2 mRNA synthesis was reactivated following demethylation, suggesting that promoter hypermethylation regulates PDSS2 transcription, which is partially consistent with our research findings and supports our study results [26].

CXCL14 is a small chemokine involved in inflammatory responses and immune regulation. In cardiac diseases, reduced expression of CXCL14 is associated with increased myocardial inflammation and fibrosis. Our findings indicate that *PDSS2* methylation inhibits the expression of *CXCL14*, leading to myocardial tissue inflammation and fibrosis, promoting the onset of heart failure. 5-azacytidine (5-Aza) is the most common demethylating agent used to block DNA methylation by forming covalent bonds [27]. Therefore, we chose 5-Aza for the treatment of HF rats. Our findings revealed that cardiac tissue from HF rats treated with 5-Aza showed significantly increased *PDSS2* level and decreased *PDSS2* methylation, confirming the inhibitory effect of 5-Aza on *PDSS2* methylation.

Additionally, we observed that a decline in CXCL14 and NF- κB expression levels accompanied the decrease in PDSS2 in HF rats. Conversely, inhibition of PDSS2 methylation by 5-Aza increased PDSS2, CXCL14, and NF- κB expression. These findings indicate that inhibiting PDSS2 expression reduced the levels of CXCL14 mRNA and protein, and inhibited the levels of NF- κB mRNA and protein. However, 5-Aza treatment reversed this phenomenon, demonstrating a significant therapeutic effect on HF. This may be attributed to the inhibition of PDSS2 methylation and restoration of PDSS2 gene expression, which effectively alleviated HF by regulating the CXCL14/NF- κB pathway.

However, this study has some limitations. Firstly, while the observed effect of PDSS2 methylation on the CXCL14/NF- κ B signaling pathway was investigated in vitro, evidence from in vivo experiments remains inadequate and full explanations about how PDSS2 methylation affects the CXCL14/NF- κ B pathway and their effects on heart failure are needed. Therefore, additional animal experiments or clinical investigations are imperative to verify the involvement of this mechanism in the pathophysiology of heart failure in humans. Secondly, the primary focus of this study was on the role of PDSS2 methylation. Subsequent research should incorporate examination of other epigenetic modifications that could potentially impact the progression of heart failure, elucidating a more comprehensive pathological framework. Finally, following studies should also investigate that whether other biological processes are involved in the *PDSS2* methylation and CXCL14/NF- κ B signaling pathway during heart failure.



Conclusion

In summary, this study reveals the significant role of *PDSS2* methylation in heart failure and preliminarily elucidates its potential mechanism in exacerbating heart failure by inhibiting the CXCL14/NF- κ B signaling pathway. These findings provide a novel perspective for investigating the molecular mechanisms of heart failure and establish a theoretical foundation for the development of innovative therapeutic approaches. Future research should further explore the role of this mechanism in heart failure and evaluate the efficacy and safety of therapeutic interventions targeting PDSS2 methylation and the CXCL14/NF- κ B signaling pathway.

Availability of Data and Materials

The original contributions presented in the study are included in the article. Further inquiries can be directed to the corresponding author.

Author Contributions

LY: Conception, Design, Materials, Data Collection, Analysis, Literature Review, Writing. SC: Design, Supervision, Materials, Data Collection, Analysis, Literature Review, Writing. XG: Supervision, Materials, Data Collection, Analysis, Writing, Critical Review. All authors read and approved the final manuscript. All authors have participated sufficiently in the work and agreed to be accountable for all aspects of the work.

Ethics Approval and Consent to Participate

This study has been approved by the Ethics Committee of Yantaishan Hospital of Shandong Province (approval no. 2021043).

Acknowledgment

Not applicable.

Funding

This research received no external funding.

Conflict of Interest

The authors declare no conflict of interest.

References

[1] Frisk M, Le C, Shen X, Røe ÅT, Hou Y, Manfra O, *et al.* Etiology-Dependent Impairment of Diastolic Cardiomyocyte Calcium Homeostasis in Heart Failure With Preserved Ejection Fraction. Journal of the American College of Cardiology. 2021; 77: 405–419.

- [2] Oikonomou E, Zografos T, Papamikroulis GA, Siasos G, Vogiatzi G, Theofilis P, *et al.* Biomarkers in Atrial Fibrillation and Heart Failure. Current Medicinal Chemistry. 2019; 26: 873–887
- [3] Güder G, Störk S. COPD and heart failure: differential diagnosis and comorbidity. Herz. 2019; 44: 502–508.
- [4] Ambrosini S, Gorica E, Mohammed SA, Costantino S, Ruschitzka F, Paneni F. Epigenetic remodeling in heart failure with preserved ejection fraction. Current Opinion in Cardiology. 2022; 37: 219–226.
- [5] Papait R, Serio S, Condorelli G. Role of the Epigenome in Heart Failure. Physiological Reviews. 2020; 100: 1753–1777.
- [6] Chen P, Zhao SH, Chu YL, Xu K, Zhu L, Wu Y, et al. Anticancer activity of PDSS2, prenyl diphosphate synthase, subunit 2, in gastric cancer tissue and the SGC7901 cell line. Anti-Cancer Drugs. 2009; 20: 141–148.
- [7] Zeng T, Tang Z, Liang L, Suo D, Li L, Li J, et al. PDSS2-Del2, a new variant of PDSS2, promotes tumor cell metastasis and angiogenesis in hepatocellular carcinoma via activating NF-κB. Molecular Oncology. 2020; 14: 3184–3197.
- [8] Kanda M, Nomoto S, Oya H, Hashimoto R, Takami H, Shimizu D, et al. Decreased expression of prenyl diphosphate synthase subunit 2 correlates with reduced survival of patients with gastric cancer. Journal of Experimental & Clinical Cancer Research. 2014; 33: 88.
- [9] Gowhari Shabgah A, Haleem Al-Qaim Z, Markov A, Valerievich Yumashev A, Ezzatifar F, Ahmadi M, et al. Chemokine CXCL14; a double-edged sword in cancer development. International Immunopharmacology. 2021; 97: 107681.
- [10] Kumar A, Mohamed E, Tong S, Chen K, Mukherjee J, Lim Y, et al. CXCL14 Promotes a Robust Brain Tumor-Associated Immune Response in Glioma. Clinical Cancer Research. 2022; 28: 2898–2910.
- [11] Zeng L, Gu N, Chen J, Jin G, Zheng Y. IRXI hypermethylation promotes heart failure by inhibiting CXCL14 expression. Cell Cycle. 2019; 18: 3251–3262.
- [12] Barnabei L, Laplantine E, Mbongo W, Rieux-Laucat F, Weil R. NF-κB: At the Borders of Autoimmunity and Inflammation. Frontiers in Immunology. 2021; 12: 716469.
- [13] Wente MN, Mayer C, Gaida MM, Michalski CW, Giese T, Bergmann F, *et al.* CXCL14 expression and potential function in pancreatic cancer. Cancer Letters. 2008; 259: 209–217.
- [14] Lu J, Song G, Tang Q, Zou C, Han F, Zhao Z, *et al.* IRX1 hypomethylation promotes osteosarcoma metastasis via induction of CXCL14/NF-κB signaling. The Journal of Clinical Investigation. 2015; 125: 1839–1856.
- [15] Liu Z, Tian H, Hua J, Cai W, Bai Y, Zhan Q, et al. A CRM1 Inhibitor Alleviates Cardiac Hypertrophy and Increases the Nuclear Distribution of NT-PGC-1α in NRVMs. Frontiers in Pharmacology. 2019; 10: 465.
- [16] Lee HC, Shiou YL, Jhuo SJ, Chang CY, Liu PL, Jhuang WJ, *et al*. The sodium-glucose co-transporter 2 inhibitor empagliflozin attenuates cardiac fibrosis and improves ventricular hemodynamics in hypertensive heart failure rats. Cardiovascular Diabetology. 2019; 18: 45.
- [17] Mori D, Miyagawa S, Matsuura R, Sougawa N, Fukushima S, Ueno T, et al. Pioglitazone strengthen therapeutic effect of adipose-derived regenerative cells against ischemic cardiomy-opathy through enhanced expression of adiponectin and modulation of macrophage phenotype. Cardiovascular Diabetology. 2019; 18: 39.
- [18] Li L, Zhong SJ, Hu SY, Cheng B, Qiu H, Hu ZX. Changes of gut microbiome composition and metabolites associated with hypertensive heart failure rats. BMC Microbiology. 2021; 21: 141.
- [19] Tahir RA, Zheng DA, Nazir A, Qing H. A review of computational algorithms for CpG islands detection. Journal of Biosciences. 2019; 44: 143.

- [20] Fukushima T, Kawaguchi M, Yamamoto K, Yamashita F, Izumi A, Kaieda T, et al. Aberrant methylation and silencing of the SPINT2 gene in high-grade gliomas. Cancer Science. 2018; 109: 2970–2979.
- [21] Svobodová Kovaříková A, Stixová L, Kovařík A, Komůrková D, Legartová S, Fagherazzi P, et al. N⁶-Adenosine Methylation in RNA and a Reduced m_3G/TMG Level in Non-Coding RNAs Appear at Microirradiation-Induced DNA Lesions. Cells. 2020; 9: 360.
- [22] Pillai-Kastoori L, Schutz-Geschwender AR, Harford JA. A systematic approach to quantitative Western blot analysis. Analytical Biochemistry. 2020; 593: 113608.
- [23] Riehle C, Bauersachs J. Small animal models of heart failure. Cardiovascular Research. 2019; 115: 1838–1849.
- [24] Abouleisa RRE, Salama ABM, Ou Q, Tang XL, Solanki M, Guo

- Y, et al. Transient Cell Cycle Induction in Cardiomyocytes to Treat Subacute Ischemic Heart Failure. Circulation. 2022; 145: 1339–1355.
- [25] Paweł K, Maria Małgorzata S. CpG Island Methylator Phenotype-A Hope for the Future or a Road to Nowhere? International Journal of Molecular Sciences. 2022; 23: 830.
- [26] Kanda M, Sugimoto H, Nomoto S, Oya H, Shimizu D, Takami H, et al. Clinical utility of PDSS2 expression to stratify patients at risk for recurrence of hepatocellular carcinoma. International Journal of Oncology. 2014; 45: 2005–2012.
- [27] Li X, Liu D, Dai Z, You Y, Chen Y, Lei C, et al. Intraperitoneal 5-Azacytidine Alleviates Nerve Injury-Induced Pain in Rats by Modulating DNA Methylation. Molecular Neurobiology. 2023; 60: 2186–2199.